Journal of ELECTRONIC MATERIALS, Vol. 45, No. 1, 2016
DOI: 10.1007/s11664-015-4146-1

Evaporation Behavior of Phosphorus from Metallurgical Grade Silicon via Calcium-Based Slag Treatment and Hydrochloric Acid Leaching

LIUQING HUANG,[1] HUIXIAN LAI,[1] CHENGHAO LU,[1] MING FANG,[1] WENHUI MA,[2] PENGFEI XING,[3] XUETAO LUO,[1,4] and JINTANG LI[1,5]

1.—Fujian Provincial Key Laboratory of Advanced Materials, College of Materials, Xiamen University, Xiamen 361005, People's Republic of China. 2.—Faculty of Materials and Metallurgical Engineering, Kunming University of Science and Technology, Kunming 650093, People's Republic of China. 3.—School of Materials and Metallurgy, Northeastern University, Shenyang 110004, People's Republic of China. 4.—e-mail: xuetao@xmu.edu.cn. 5.—e-mail: leejt@xmu.edu.cn

Phosphorus removal from metallurgical grade silicon by CaO-SiO_2-$CaCl_2$ slag treatment, HCl leaching, and vacuum refining was investigated. The effect of different compositions of slag was evaluated. The calcium concentration in slag-treated silicon increased with increasing CaO/SiO_2 mass ratio of slag, decreasing the evaporation efficiency of phosphorus in molten silicon. The total phosphorus removal efficiency changed from 93.0% to 98.3% when the slag-treated silicon was treated with HCl before vacuum refining. The final concentration of phosphorus in silicon was 0.43 ppmw. This is because phosphorus was removed from metallurgical-grade silicon as follows: Phosphorus reacts with slag at the silicon/slag interface and forms $Ca_3(PO_4)_2$ and Ca_3P_2, most of which diffuse from the interface to the slag phase. The remaining $Ca_3(PO_4)_2$ and Ca_3P_2 reduce the phosphorus removal efficiency by altering the activity coefficient of phosphorus in molten silicon. HCl leaching enhanced the phosphorus removal efficiency by removing the remaining $Ca_3(PO_4)_2$ and Ca_3P_2. Therefore, the mass transfer of phosphorus from metallurgical-grade silicon was accelerated.

Key words: Metallurgical-grade silicon, slag treatment, acid leaching, vacuum refining, phosphorus evaporation

Abbreviations

MG-Si	Metallurgical-grade silicon
SoG-Si	Solar-grade silicon
Si-S	45 wt.% CaO-45 wt.% SiO_2-10 wt.% $CaCl_2$ slag treated MG-Si sample
Si-S-L	HCl-leached Si-S sample
Si-S-L-V	Vacuum-refined Si-S-L sample
Si-S-V	Vacuum-refined Si-S sample
ppmw	Parts per million weight

(Received December 21, 2014; accepted October 10, 2015; published online November 18, 2015)

INTRODUCTION

The demand for clean and renewable resources has been increasing with recent advances in photovoltaic technology. Metallurgical-grade silicon (MG-Si, purity 99 wt.%), the raw material for solar cells, is extensively used in the photovoltaic industry. Therefore, much attention has been paid to upgrade MG-Si to solar-grade silicon (SoG-Si, purity 99.9999 wt.%) by metallurgical routes.[1,2] Previous studies have shown that most metallic impurities such as Fe, Al, Ca, Mn, and Ti can be easily removed by directional solidification, owing to their small segregation coefficients.[3] Nevertheless, boron and phosphorus, the major nonmetallic impurities in MG-Si, cannot be effectively removed by directional solidification because of their relatively large segregation coefficients.[4]

Because phosphorus has a high saturated vapor pressure in molten silicon (P_P = 59,914.43 Pa at 1873 K),[5] vacuum refining[6] and electron-beam methods[7,8] are excellent for removing phosphorus from MG-Si; for example, the concentration of phosphorus was reduced by 0.08 ppmw and 0.07 ppmw,[9] respectively. However, the individual processes have their own limitations, causing a much higher total concentration of impurities than the acceptable concentration. Therefore, it is essential to combine different processes to produce SoG-Si from MG-Si. In recent years, studies have combined different processes to remove impurities with great efficiency. The studies have shown that pretreatment before phosphorus evaporation significantly affects the position and state of phosphorus in MG-Si. Solvent refining is one of the most widely used methods for MG-Si purification. Wang et al.[10] reported that phosphorus was removed effectively by solvent refining and acid leaching because of a decrease in the segregation coefficient of phosphorus in Sn-Si and Al-Si systems. Min and Sano[11] reported that calcium has a great affinity for phosphorus, indicating that phosphorus probably formed impurity phases with calcium. Johnston et al.[12] alloyed calcium with silicon to form a minor phase in order to attract phosphorus, thus removing the impurities. Ludwig et al.[13] studied the effect of calcium addition on Si-Al alloy in the presence of phosphorus at different concentrations; calcium stabilized the state of phosphorus in Si-Al alloy thermodynamically. However, separation of the alloy phases and the purified silicon phase requires rigorous equipment and consumes high energy. Another notable process is slag treatment. As a practical and economical method for removing impurities, slag treatment has been combined with a metallurgical route. Calcium-based slag and sodium-based slag are most widely used. Several studies have reported that the basicity of slag, fluxes, and active reagents affects the removal efficiency of impurities.[14–16] Tagaya et al.[17] reported the thermodynamic behavior of phosphorus in CaO-CaF_2-SiO_2 and Na_2O-CaO-SiO_2 systems. Jung et al.[18] reported that the stability of phosphorus in slag depends on both the basicity of slag and the solubility of calcium in silicon. Meteleva-Fischer et al.[19] reported that the phosphorus present in the grain-boundary phase of silicon was removed after slag treatment, along with most metallic impurities by acid leaching.

Previous studies on MG-Si purification mostly involved the removal of impurities by individual or combined processes. However, the relationship between process characteristics, the nature of the microstructure, elemental distribution, and mass transfer parameters has been rarely investigated. Therefore, in this study, the effect of slag treatment and acid leaching on phosphorus evaporation after vacuum refining was evaluated to better understand the MG-Si purification mechanism for optimizing the removal efficiency of impurities. The removal efficiency of phosphorus and other impurities was determined by inductively coupled plasma atomic emission spectrometry (ICP-AES). Moreover, each process was studied by scanning electron microscope/energy dispersive spectroscopy (SEM–EDS), and elemental distribution was analyzed using an electron probe microanalyzer (EPMA). Furthermore, the mechanism of phosphorus removal using the combined processes was also elucidated.

EXPERIMENTAL

Materials

MG-Si with a purity of 99 wt.% was purchased from Run Xiang Co., Ltd., China. The slag compositions used in the experiments are listed in Table I. The slags consisted of analytical-grade CaO powder, SiO_2 powder, and $CaCl_2$ powder; the powders were mixed thoroughly by mechanical stirring. Reagent-grade HCl was used in acid leaching experiments. The reagents were purchased from Sinopharm Chemical Reagent Co., Ltd.

Methods

Figure 1 shows the purification process of MG-Si schematically. In the slag treatment experiment, an intermediate frequency induction melting furnace with a high-frequency power supply (10 kV) and heating elements was used. A high-strength and high-purity graphite crucible was placed inside the furnace using a carbon holder. Temperature was measured using a WRe5-WRe26 thermocouple and controlled within ±10 K. According to the volume of the crucible and the densities of the slag composition, the total mass in each group was maintained at 120 g. In the slag treatment experiment, 60 g MG-Si and 60 g CaO-SiO_2-$CaCl_2$ slag were mixed in the graphite crucible and melted in an argon atmosphere. After the slag treatment, the melt was cooled down, and the treated silicon was separated from the slag by mechanical crushing at room temperature. In the vacuum refining experiment, a vacuum melting furnace was used. Twenty grams of the preliminarily purified silicon was melted directly under vacuum. The concentration of phosphorus in MG-Si was usually 10–50 ppmw; therefore, it was difficult to confirm the mass transfer of a trace amount of phosphorus in MG-Si. To determine the distribution of phosphorus after each procedure, a Si-P melt was prepared. First, 100 g MG-Si and 10 g red phosphorus were mixed and then melted at 1773 K for 30 min. The final phosphorus concentration was 7777 ppmw. The Si-P alloy sample was ground and mixed with 45 wt.% CaO-45 wt.% SiO_2-10 wt.% $CaCl_2$ slag (alloy/slag mass ratio = 1:1). The slag treatment was carried out at 1923 K for 30 min using the intermediate frequency inductive furnace. Twenty grams of the

Table I. Compositions of CaO-SiO_2-$CaCl_2$ slag equilibrated with MG-Si

Series	Initial composition of slag (wt.%)			CaO/SiO_2	Optical basicity	Slag/MG-Si
	CaO	SiO_2	$CaCl_2$			
1	40	50	10	0.8	0.69	1.0
2	45	45	10	1.0	0.75	1.0
3	50	40	10	1.25	0.80	1.0
4	55	35	10	1.57	0.86	1.0
5	60	30	10	2.0	0.90	1.0

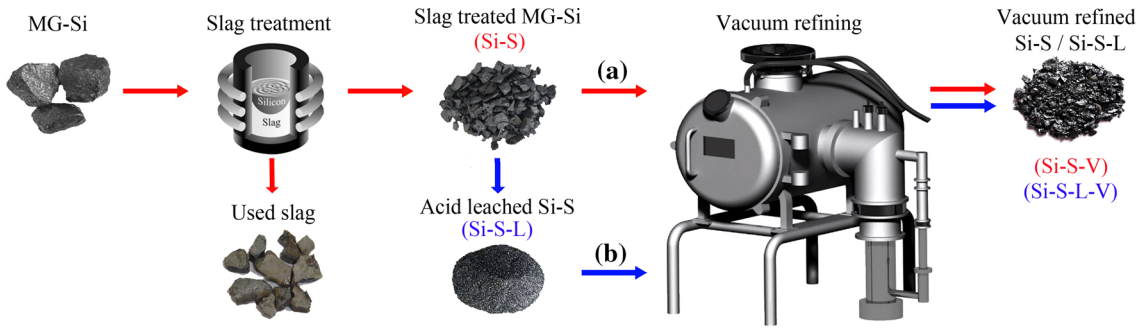

Fig. 1. Schematic purification process of MG-Si. (a) The Si-S-V sample was obtained by 45 wt.% CaO-45 wt.% SiO_2-10 wt.% $CaCl_2$ slag treatment and vacuum refining with MG-Si. (b) The Si-S-L-V sample was obtained by 45 wt.% CaO-45 wt.% SiO_2-10 wt.% $CaCl_2$ slag treatment, HCl leaching, and vacuum refining with MG-Si.

Table II. Melting conditions in slag treatment and vacuum refining

Process	Melting parameter	Value
Slag treatment	Treatment temperature (K)	1923
	Treatment time (min)	30
	Atmosphere	Argon
Vacuum refining	Refining temperature (K)	1823
	Melting time (min)	180
	Chamber pressure (Pa)	<0.1

preliminarily purified silicon was treated with HCl in a Teflon beaker at room temperature for 12 h before the vacuum refining. The H^+ concentration was 5 M, and the solid-to-liquid weight ratio was fixed at 1:10. After acid leaching, the residues were filtered and washed with deionized water using an ultrasonic cleaner before the drying. The detailed experimental parameters are given in Table II.

Analysis

The concentration of impurities in the MG-Si and Si-P melt was measured by ICP-AES (Optima 2000DV, PerkinElmer Inc., US). The surface morphology of specimens and the composition of precipitated phases before and after each procedure were analyzed by SEM–EDS (Cambridge S360, Cambridge, U.K.). The elemental distribution in the Si-P melt after slag treatment was analyzed using an EPMA (JXA-8100, Japan Electronics Co. Ltd., Japan). The surface of specimens was analyzed by x-ray photoelectron spectroscopy (XPS, PHI Quantum 2000, Physical electronics Co. Ltd., USA). The surface morphology of the slag-treated MG-Si powder before and after acid leaching, and vacuum refining was observed using SEM (SU70, Hitachi Co. Ltd., Japan).

RESULTS

Effect of Slag Treatment on Phosphorus Removal

The effect of slag treatment on phosphorus evaporation from MG-Si was evaluated by varying the

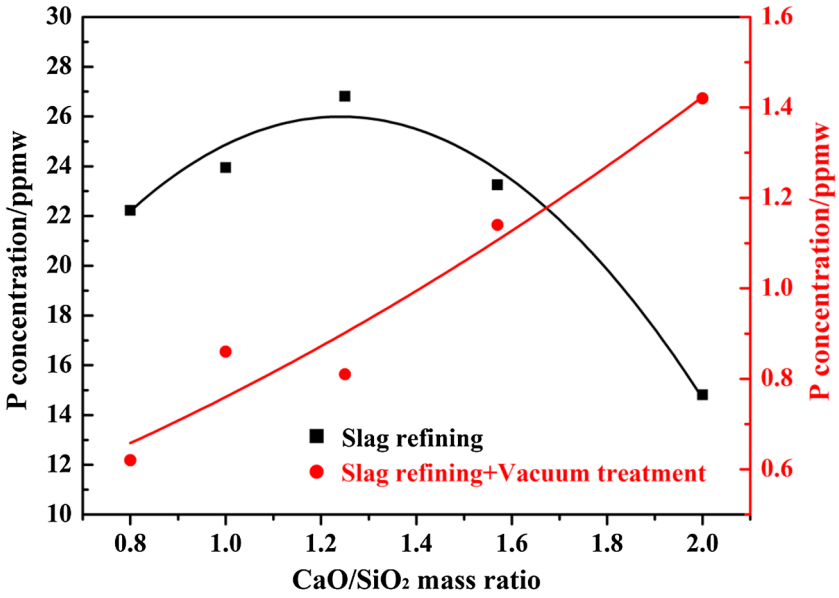

Fig. 2. Relationship between CaO/SiO_2 mass ratio and phosphorus concentration after $CaO\text{-}SiO_2\text{-}CaCl_2$ slag treatment and subsequent vacuum refining.

CaO/SiO_2 mass ratio from 0.8 to 2.0. The $CaCl_2$ content was fixed at 10 wt.%. Figure 2 shows that with the increase in CaO/SiO_2 mass ratio, the phosphorus concentration after the slag treatment first increased and then decreased, reaching a maximum phosphorus concentration of 26.81 ppmw when the CaO/SiO_2 mass ratio was 1.25. However, the phosphorus concentration increased with an increase in the CaO/SiO_2 mass ratio in the subsequent vacuum refining.

A Si-P melt was prepared to determine the elemental distribution, and its phosphorus concentration was 7777 ppmw. Based on the Si-P system in the Si-rich domain,[20] the Si-P melt was regarded as a pure substance because its phosphorus concentration was in the ppmw range. Figure 3 shows the microstructure of the Si-P sample before and after the 45 wt.% CaO-45 wt.% SiO_2-10 wt.% $CaCl_2$ slag treatment (Si-P-S) and vacuum refining (Si-P-S-V). The chemical compositions of different colored precipitates are shown in Fig. 3. The darker area is the silicon phase, and the lighter area is the precipitated impurities phase. The EDS quantitative analysis data and chemical compositions are shown in Table III. Si-P-Fe based compounds precipitated in the impurity phase of Si-P melt as shown in Fig. 3a. Figure 3b shows that calcium accumulated in the precipitated phase after the slag treatment. Figure 3c shows another feature of the remaining Si-Ca-Fe phase. The phosphorus concentration reduced substantially, below the detection limit, after vacuum refining.

The full XPS spectra of the Si-P and Si-P-S samples are shown in Fig. 4a to determine if Ca-P-containing compounds existed after slag treatment. As shown in Fig. 4a, the appearance of the Ca peak in the Si-P-S sample was different from that in the Si-P sample. The corresponding P 2*p* peaks of the Si-P and Si-P-S sample are shown in Fig. 4b. Before the slag treatment, the P 2*p* peak of the Si-P sample was located at 133.0 eV, whereas the P 2*p* peak of the Si-P-S sample could be deconvoluted into two separate peaks. The most intense peak was located at 133.0 eV and the second intense peak was centered at 136.2 eV, thus shifting the peak to a higher binding energy. This indicates the P-O bonding in $PO4^{3-}$; therefore, some amount of phosphorus may have been oxidized to $Ca_3(PO_4)_2$.

To better investigate the elemental distribution of the Si-P sample, the EPMA mapping images were recorded. The distribution of Si, Ca, O, and P in Si-P melt after the slag treatment is shown in Fig. 5. Notably, parts of P-rich position overlapped with the Ca and O-rich positions after slag treatment of the Si-P melt. This is consistent with the results of XPS analysis; thus, Ca-P-containing compounds were formed after treating with 45 wt.% CaO-45 wt.% SiO_2-10 wt.% $CaCl_2$ slag.

Effect of Acid Leaching on Phosphorus Removal in Slag-Treated MG-Si

In this study, an additional MG-Si acid leaching experiment was conducted for slag-treated MG-Si before vacuum refining. Shimpo and Morita et al.[21,22] reported that the addition of calcium improved the removal efficiency of phosphorus in silicon via acid leaching. Unlike Shimpo's work, in this study, the calcium was derived from Ca-based slag treatment instead of adding to MG-Si directly. The

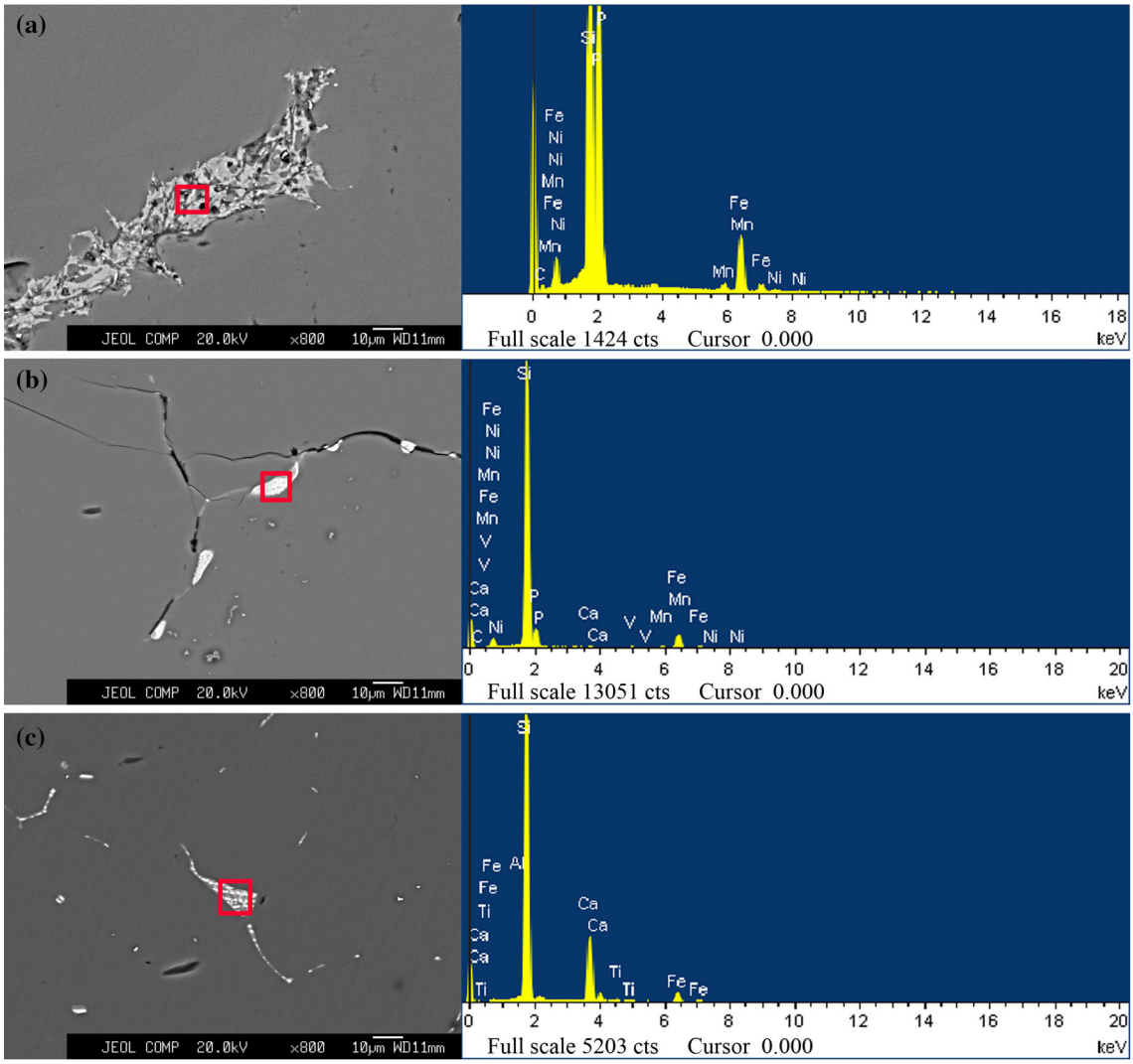

Fig. 3. Microstructure of the precipitated phase in (a) Si-P, (b) Si-P-S and (c) Si-P-S-V, and the corresponding EDS analysis.

Table III. EDS quantitative analysis and chemical composition of the impurity phase

	Major element/atomic percent						
Samples	**Si**	**P**	**Ca**	**Fe**	**Mn**	**Ni**	**Composition of phase**
Si-P	42.28	30	–	6.02	0.61	0.33	Si-P-Fe
Si-P-S	69.61	8.87	0.25	8.26	1.05	0.44	Si-P-Fe-Mn
Si-P-S-V	71.39	–	21.82	5.27	0.21	0.15	Si-Ca-Fe

– indicates a concentration below the detection limit.

effect of acid leaching on the impurity removal efficiency R_E and the total impurity removal efficiency R_T was investigated, and the results are shown in Fig. 6. Here, the impurity removal efficiency R_E and the total impurity removal efficiency R_T are defined as Eqs. 1 and 2, respectively.

$$R_E = \left(1 - \frac{\text{remaining element concentration in purified Si}}{\text{element concentration in raw MG} - \text{Si}}\right) \times 100\% \quad (1)$$

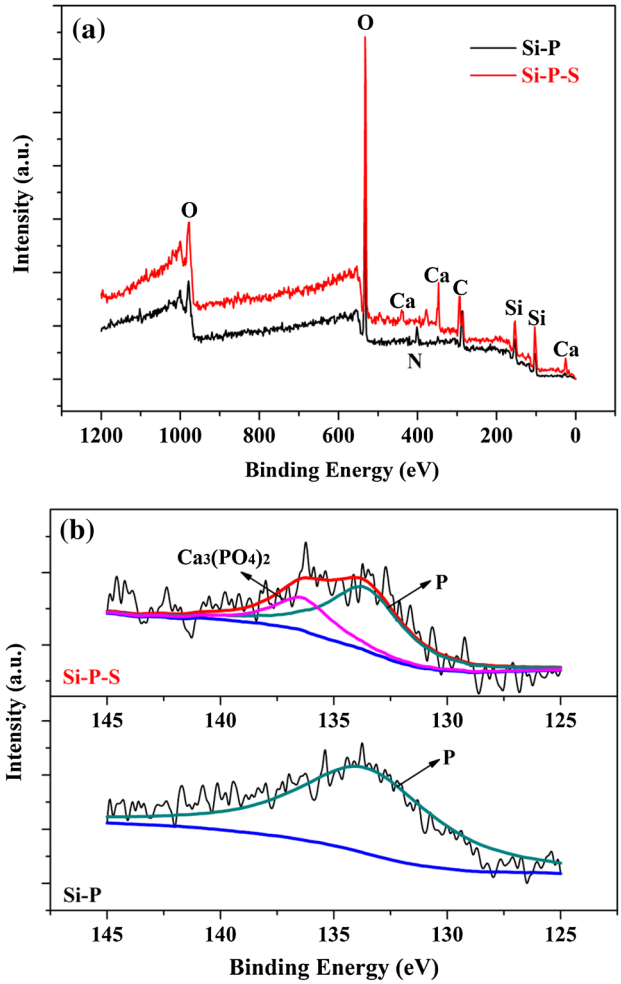

Fig. 4. (a) Full XPS spectra and (b) P 2*p* (124–144 eV) regions of Si-P and Si-P-S samples.

$$R_T = \left(1 - \frac{\text{remaining total impurities concentration in purified Si}}{\text{total impurities concentration in raw MG} - \text{Si}}\right) \times 100\% \quad (2)$$

Figure 6 shows the effect of acid leaching on the total removal efficiency of each impurity. The calcium introduced by calcium-based slag was effectively removed after the acid leaching and the R_{ca} value increased from 74.9% to 99.2%. Moreover, the phosphorus concentration decreased from 0.86 ppmw to 0.43 ppmw, whereas the R_P value increased from 93.0% to 98.3%. It was beneficial for removing all other impurities, particularly Fe, Al, and Ti. Table IV shows the major impurity concentrations after each procedure.

Morphology and Elemental Distribution of MG-Si for Each Process

Figure 7 shows the morphologies of the milled powder and polished surface of MG-Si after the slag treatment, acid leaching, and vacuum refining. Figure 7a shows some residues on the surface of slag-treated Si powders, and the residue consists of Si, Ca, O, and Cl, the same as in the CaO-SiO_2-$CaCl_2$ slag composition. Thus, it can be concluded that the residue originated from the slag. Moreover, numerous scrapes and grooves were observed on the surface of MG-Si after the slag treatment. This change can be attributed to the rapid temperature change, resulting in large stresses. This caused many cracks and defects along the grain boundaries and produced some scrapes. Therefore, the impurities were exposed on the surface of silicon, which was beneficial for removing them using acid leach-

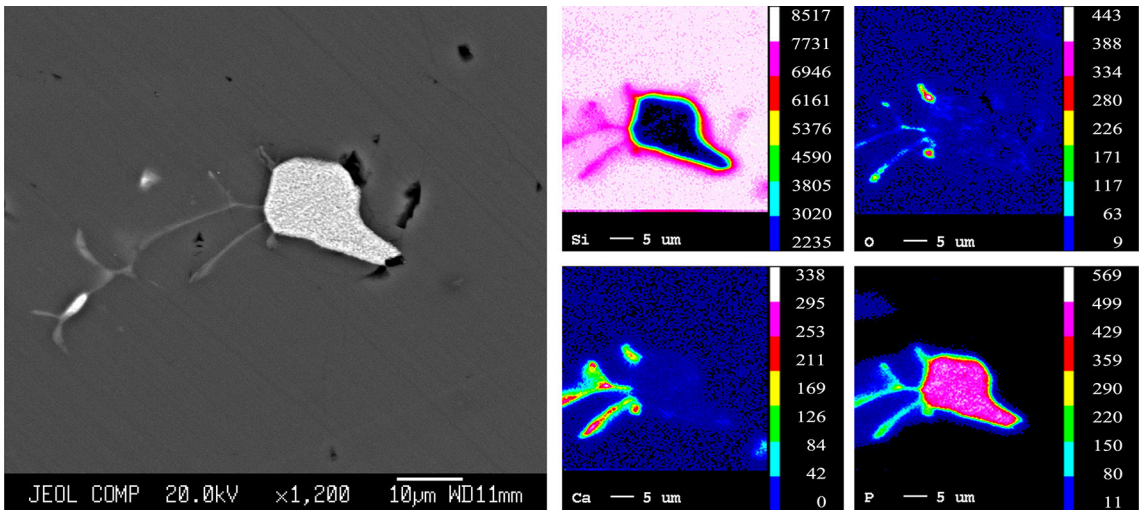

Fig. 5. Distribution of Si, Ca, P, and O in the impurity phase from 45 wt.% CaO-45 wt.% SiO_2-10 wt.% $CaCl_2$ slag-treated Si-P melt.

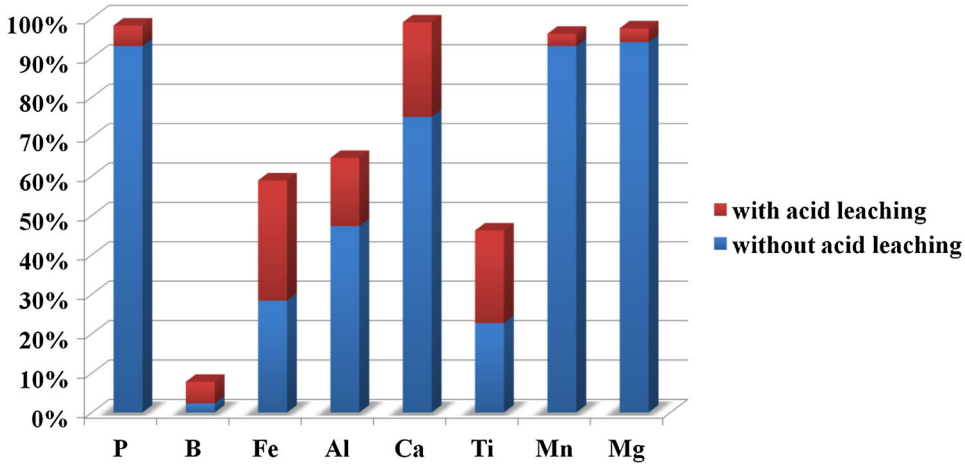

Fig. 6. Effect of HCl leaching on the total removal efficiency of each impurity elements in MG-Si. The leaching experiments were carried out on the <149 μm fraction of MG-Si after slag treatment with 5 M HCl at room temperature for 12 h.

Table IV. Leaching results for each procedure

	MG-Si	Slag treatment	Acid leaching	Vacuum refining
P concentration (ppmw)	25.27	23.94	20.73	0.43
Total impurities concentration (ppmw)	2240.54	4617.81	1665.9	613.74
P removal efficiency (%)	–	5.26	17.97	98.30
Total removal efficiency (%)	–	–	25.65	72.61
Purity (%)	99.7759	99.5382	99.8334	99.9386

Table V. Possible reactions of phosphorus during CaO-based slag treatment

Reactions	ΔG (J/mol)	Temp. (K)	References	Equation no.
$(SiO_2) = (Si) + O_2(g)$	$947{,}434 - 201T$	1723–1823	23	3
$(CaO) + 0.5[Si] = 0.5(SiO_2) + [Ca]$	$156{,}000 - 20T$	1823/1873	24	4
$0.5P_2(g) = [P]$	$-139{,}000 + 43T$	1723–1848	25	5
Oxidation				
$2[P] + 2.5O_2(g) = (P_2O_5)$	$-1{,}499{,}597 + 571T$	1823–1923	26	6
$2[P] + (SiO_2) = (P_2O_5) + (Si)$	$915{,}720 - 88.3T$	1773–1873	27	7
$0.5P2(g) + 1.25O2(g) + 1.5CaO = 0.5(Ca_3(PO_4)_2)$	$-1{,}084{,}106 + 278T$	1773	28	8
Reduction				
$2P_2(g) + (CaO) = (Ca_3P_2) + 3O_2(g)$	$608{,}261 - 43T$	1723–1823	23	9

[], (), and (g) represent the metal, slag, and gas phases, respectively.

ing. The EDS quantitative analysis of the polished surface showed that the main precipitated phase was the Si-Ca-Fe-Mn phase. After the acid leaching, the surface of MG-Si particles was cleaner than the slag-refined silicon, as shown in Fig. 7b. The amount of metallic impurities, namely, Ca, Ti, Mn, Fe, and Ni, was less than that of the slag-treated silicon. This indicates that the acid leaching was effective for removing the metallic impurities exposed on the grain surface. The acid-leached MG-Si powders were remelted under vacuum. As shown in Fig. 7c, vacuum refining was effective for removing calcium, which has a larger saturated pressure than silicon. Furthermore, the Si-Fe phase was the main precipitated phase.

DISCUSSION

Mass Transfer of Phosphorus During Slag Treatment

The removal of phosphorus from silicon by slag treatment is a complex process, and the main

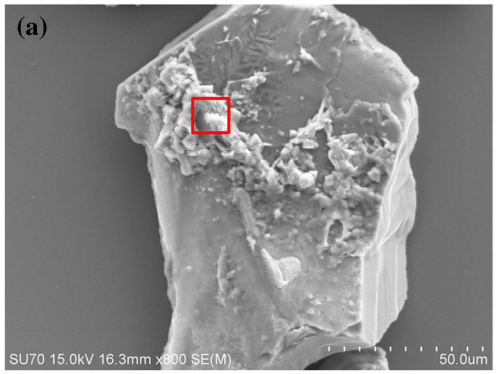

Element	Weight %	Atomic %
O K	46.45	61.27
Si K	46.68	35.08
Cl K	0.55	0.33
Ca K	6.12	3.32
Totals	100.00	

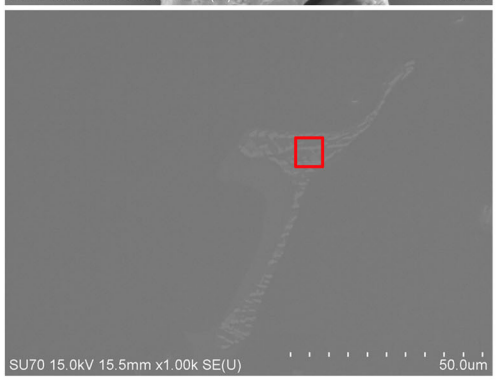

Element	Weight %	Atomic %
Al K	0.30	0.35
Si K	70.90	80.78
Ca K	9.71	7.75
Ti K	1.31	0.87
V K	0.83	0.52
Mn K	3.16	1.84
Fe K	12.79	7.33
Ni K	1.00	0.56
Totals	100.00	

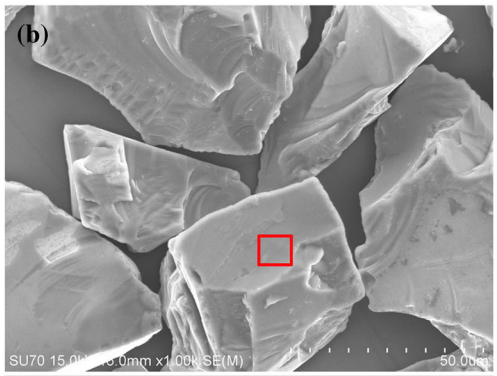

Element	Weight %	Atomic %
O K	1.28	2.22
Si K	98.72	97.78
Totals	100.00	

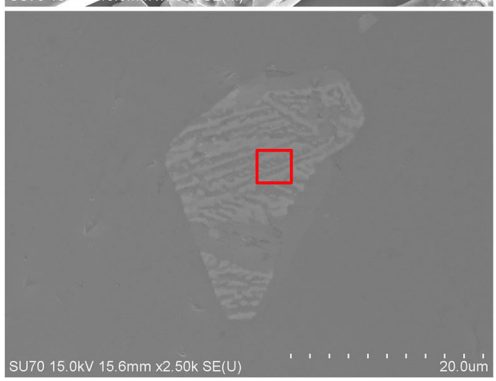

Element	Weight %	Atomic %
O K	1.78	3.15
Si K	93.28	93.77
Ca K	2.87	2.02
Ti K	0.24	0.14
Mn K	0.29	0.15
Fe K	1.16	0.59
Ni K	0.38	0.18
Totals	100.00	

Fig. 7. SEM images of the milled particles and polished surface of the three varieties of refined MG-Si: (a) Si-S; (b) Si-S-L; and (c) Si-S-L-V.

mechanism involved is oxidation reaction, which has not yet been clarified. In this study, the removal mechanism was elucidated. We assume that phosphorus was first oxidized or reduced at the silicon/slag interface and then transferred into the slag phase during slag treatment. The possible reactions reported by several studies are shown in Table V, and the corresponding mechanisms are as follows:

The possibility of phosphorus removal by oxidation was evaluated. Slag treatment usually removes impurities by oxidation. In general, the phosphorus present in the molten silicon is first oxidized in the slag phase as

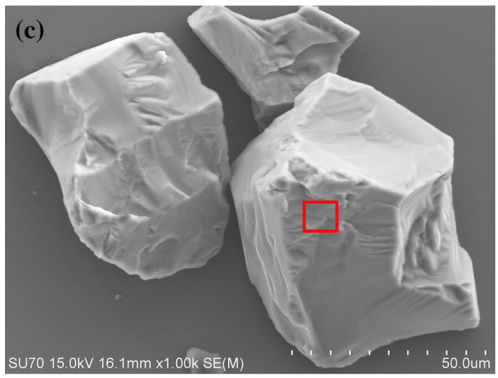

Element	Weight %	Atomic %
O K	0.67	1.17
Si K	99.33	98.83
Totals	100.00	

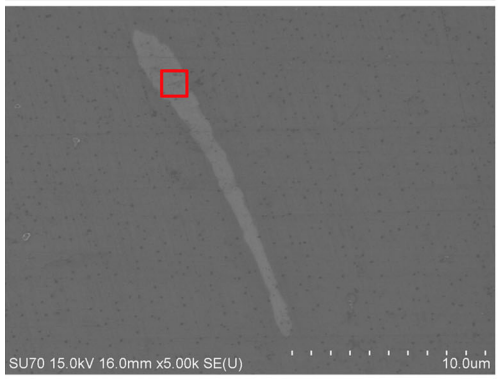

Element	Weight %	Atomic %
O K	4.09	7.85
Si K	72.01	78.74
Ca K	0.73	0.56
Ti K	1.35	0.86
V K	0.69	0.42
Fe K	19.50	10.72
Ni K	1.63	0.86
Totals	100.00	

Fig. 7. continued.

P_2O_5 and then reacts with CaO to form $Ca_3(PO_4)_2$, as expressed by Eqs. 3–9. Notably, the affinity between Ca and O_2 is stronger than that between Mg, Al, Si, Mn, P, and Fe, according to the Ellingham diagram for oxide.[29] Therefore, it is more likely that phosphorus oxidation occurred along with silicon oxidation. This indicates that oxidation may not be the only method to remove phosphorus impurity, consistent with that reported by Jung et al.[27] Dephosphorization rarely occurs because the Gibbs energy of forming P_2O_5 is strongly positive.

The possibility of phosphorus removal by reduction was also evaluated. The partial pressure of oxygen corresponding to the Si/SiO_2 equilibrium between the slag and silicon at the interface was determined by the silicothermic reduction reaction (4). Because calcium has a small activity in liquid silicon and SiO_2 is more stable than CaO, reaction (4) is possible through the contact of silicon and the slag. The general reaction between phosphorus (in the form of $P_2(g)$) and other impurity elements can be expressed as Eq. 10 (M = Ca, Fe, Al, etc.).

$$2x/y[\mathrm{M}] + \mathrm{P_2(g)} = 2/y\left(\mathrm{M}_x\mathrm{P}_y\right). \tag{10}$$

The Gibbs free energy changes for the possible reaction of P_2 in molten silicon in the range of 1273–2273 K are shown in Fig. 8. The calculations were carried out using the HSC Chemistry version 7.0 software (Outokumpu Research Oy, Pori, Finland). Among the seven possible reactions shown in Fig. 7, there were two reactions that had a high negative ΔG at 1923 K:

$$[\mathrm{Ca}] + \mathrm{P_2(g)} \rightarrow \mathrm{Ca_3P_2} \tag{11}$$

$$[\mathrm{Mg}] + \mathrm{P_2(g)} \rightarrow \mathrm{Mg_3P_2}. \tag{12}$$

Thus, it can be concluded that Ca and Mg have great potential for forming phosphide during the slag treatment. However, MG-Si has a low concentration of Mg; therefore, reaction (12) can be ignored.

Mass Transfer of Phosphorus During Acid Leaching Process

Jung et al.[18] reported that the calcium concentration in silicon increased with increasing CaO activity, and Ca-P compounds can be removed by acid leaching. Fang et al.[30] reported that HCl showed a good phosphorus removal efficiency for slag-treated MG-Si. In this study, acid leaching was carried out using HCl at room temperature for slag-treated MG-Si before the vacuum refining. The removal efficiencies of calcium and phosphorus were found to be 67.0% and 13.4%, respectively. Although the phosphorus concentration was low, it was confirmed that an amount of Ca-P-containing compound was removed by acid leaching. Most of the calcium reacts with Si to form $CaSi_2$, which is acid soluble. This can be explained by the leaching mechanism as follows:

The removal of impurities from MG-Si by treating with HCl can be expressed by Eqs. 13–15.

$$Ca_3(PO_4)_2(s) + 6HCl(aq.) = 3CaCl_2(l) + 2H_3PO_4(l), \quad (13)$$

$$Ca_3P_2(s) + 12HCl(aq.) = 3CaCl_2(l) + 2PCl_3(l) + 6H_2(g), \quad (14)$$

$$2CaSi_2(xFe, yAl)(s) + (4x + 6y + 20)HCl(aq.) = 2CaCl2(l) + 4SiCl_4(l) + 2xFeCl_2(l) + 2yAlCl_3(l) + (2x + 3y + 10)H_2(g). \quad (15)$$

Moreover, based on the cracking shrinking model,[31] HCl has a cracking effect on MG-Si. The preliminary refined silicon was beneficial for vacuum refining in the powdered form, thus facilitating phosphorus evaporation. Therefore, acid leaching may be effective for removing phosphorus.

Mass Transfer of Phosphorus During Vacuum Refining

During vacuum refining, the phosphorus present in the silicon melt was transferred from the melt to the gas phase. First, the phosphorus was transferred from the melt to the melt surface. Then, the phosphorus was evaporated from the melt in the liquid/gas interface. Finally, the phosphorus was removed from the interface in the gas phase and extracted by the vacuum system.

Phosphorus Transportation from the Melt to the Boundary Layer

Considering that the silicon melt or droplet was subjected to electromagnetic stirring, Machlin's rigid flow theory[32] can be applied to describe the mass transfer of phosphorus in molten silicon. The mass transfer coefficient of phosphorus under convection condition can be expressed as follows:

$$K_D = \sqrt{\frac{8DV_m}{\pi r}}, \quad (16)$$

where D is the diffusion coefficient of phosphorus in the molten silicon ($D = 2 \times 10^{-7}$ exp(−17,700/RT) m^2/s[33]), V_m is the average surface velocity of the melt (V_m = 0.182 m/s[34]), R is the universal gas constant (R = 8.134 J/mol K), and r is the melt radius (r = 0.095 m[35]). K_D was taken as a constant when the temperature reached 1823 K and calculated as $K_D = 1.01 \times 10^{-3}$ m/s.

Phosphorus Evaporation from the Melt into the Gas Phase

The dephosphorization reaction follows first-order kinetics. The evaporation mass transfer coefficient K_E can be expressed using Eq. 17.[36]

$$K_E = \frac{100P_a\gamma_{P\text{ in Si}}\exp\left(-\frac{\Delta G^0}{RT}\right)}{\rho_{Si}}\sqrt{\frac{M_P}{2\pi RT}}, \quad (17)$$

where P_a is the atmospheric pressure (P_a = 101,325 Pa), ΔG^0 is the Gibbs energy change of phosphorus from the melt into the gas phase (ΔG^0 = 387,000–103T J/mol), T is the temperature (T = 1823 K), ρ_{Si} is the density of Si (ρ_{Si} = 2500 kg/m^3), M_P is the molar mass of phosphorus ($M_P = 3.097 \times 10^{-2}$ kg/mol) and $\gamma_{P\text{ in Si}}$ is the activity coefficient of phosphorus in the molten silicon as expressed using Eq. 18, taken as 1 in theoretical simulation, K_E was taken as a function of $\gamma_{P\text{ in Si}}$ when the temperature reached 1823 K, and was calculated as $K_E = 4.516 \times 10^{-6}\ \gamma_{P\text{ in Si}}$ m/s.

$$\ln\gamma_{P\text{ in Si}} = \ln\gamma^0_{P\text{ in Si}} + \varepsilon^P_{P\text{ in Si}}x_{P\text{ in Si}} + \varepsilon^{Ca}_{P\text{ in Si}}x_{P\text{ in Si}}, \quad (18)$$

where $\gamma^0_{P\text{ in Si}}$ is the activity coefficient of silicon in the molten calcium at infinite dilution relative to pure liquid silicon, $\varepsilon^P_{P\text{ in Si}}$ is the self-interaction parameter of phosphorus in molten silicon, and $\varepsilon^{Ca}_{P\text{ in Si}}$ is the interaction parameter between calcium and phosphorus in molten silicon.

Thus, the overall mass transfer coefficient of phosphorus, K_P (m/s), can be calculated using Eq. 19. Because the K_P is proportional to K_E, K_P increased with the increase in $\gamma_{P\text{ in Si}}$.

$$\frac{1}{K_P} = \frac{1}{K_D} + \frac{1}{K_E}. \quad (19)$$

The evaporation of phosphorus follows first-order kinetics. The impurity concentration in the liquid phase can be expressed as a function of the melting time t(s) as follows:

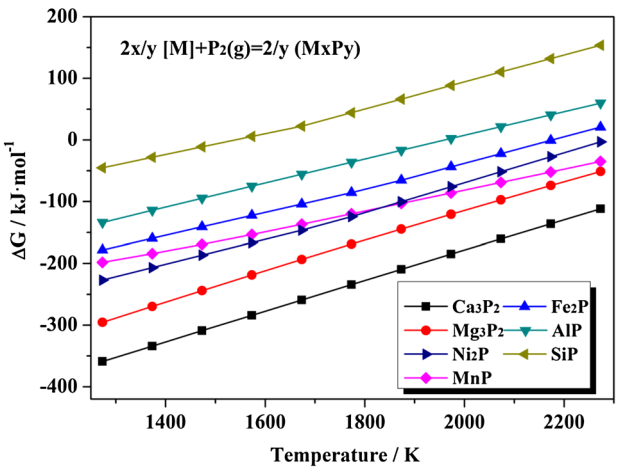

Fig. 8. Standard Gibbs free energy changes in phosphide for the impurities in MG-Si at a temperature of 1273–2273 K.

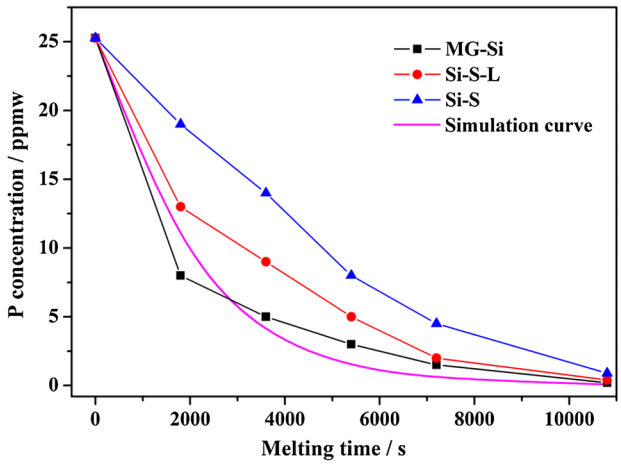

Fig. 9. Changes in phosphorus concentration in vacuum-refined MG-Si, Si-S-L, and Si-S samples and the comparison of experimental data with the simulation curve. Vacuum refining temperature = 1823 K, chamber pressure < 0.1 Pa.

$$\frac{dW_p}{dt} = -\frac{A}{V}K_P W_P, \quad (20)$$

where V (m^3) is the volume, A (m^2) is the melt surface, W_P is the mass percentage of phosphorus in the molten silicon at $t = 0$ s and $t = t$ s. Rearranging Eq. 20, the following expression can be obtained. Therefore, the concentration of phosphorus is time-variant when A, V and K_P were taken as constants.

$$\frac{WP_t}{WP_0} = \exp\left[-\frac{A}{V}K_P(t - t_0)\right]. \quad (21)$$

Comparison of the Experimental and Simulation Results of Phosphorus Removal

To validate the effects of slag treatment and acid leaching on the phosphorus evaporation in MG-Si, comparison experiments were carried out by melting the MG-Si sample, 45 wt.% CaO-45 wt.% SiO_2-10 wt.% $CaCl_2$ slag-treated MG-Si sample (Si-S) and HCl-treated Si-S sample (Si-S-L) under vacuum with varying time.

As shown in Fig. 9, the experimental results show a similar trend as the simulation curve. The evaporation potential of phosphorus in MG-Si was found to be greater than Si-S-L and Si-S when the refining time was fixed at 180 min, and the concentrations of phosphorus in MG-Si, Si-S-L, and Si-S were 0.21 ppmw, 0.43 ppmw, and 0.92 ppmw, respectively. According to the above analysis and discussion, a large amount of calcium was recovered from the CaO in the silicon melt after the slag treatment. Miki et al. reported that calcium affected the activity of phosphorus in MG-Si.[25] Equation 18 shows that $\gamma_{P\,in\,Si}$ first decreased with the increase in calcium concentration in molten silicon and then affected the evaporation of phosphorus from molten silicon. The phosphorus evaporation efficiency decreased with the increase in CaO/SiO_2 mass ratio, as shown in Fig. 2. This indicates that an increase in the calcium concentration in MG-Si will decrease the phosphorus evaporation potential. Therefore, MG-Si has an optimum phosphorus evaporation potential, whereas the evaporation potential of Si-S was the worst. The experimental data for MG-Si agreed well with the simulation curve. The experimental data of Si-S-L lay between that of MG-Si and Si-S. This is because Ca-P-containing compounds were removed by acid leaching, thus facilitating phosphorus evaporation. The experimental data fit well with the theoretical prediction.

CONCLUSIONS

A purification process for MG-Si was developed by combining $CaO\text{-}SiO_2\text{-}CaCl_2$ slag treatment, HCl leaching, and vacuum refining. The results show that the evaporation efficiency of phosphorus decreased with an increase in the CaO/SiO_2 mass ratio. Some amount of phosphorus was found to concentrate in the Ca-rich area, indicating that the phosphorus in MG-Si existed in the form of $Ca_3(PO_4)_2$ and Ca_3P_2 after the slag treatment. Because the calcium present in the molten silicon decreased the evaporation ability of phosphorus by decreasing the activity coefficient of phosphorus, $Ca_3(PO_4)_2$ and Ca_3P_2 were removed by treating with acid before the vacuum refining. The total calcium removal efficiency increased from 74.9% to 99.2%, and the phosphorus concentration decreased from 25.27 ppmw to 0.43 ppmw. The total phosphorus removal efficiency increased from 93.0% to 98.3%. Moreover, acid leaching was beneficial for evaporating phosphorus from MG-Si in powdered form. The evaporation potential of phosphorus in MG-Si, Si-S, and Si-S-L samples was evaluated under vacuum. The experimental results show a similar trend as the theoretical simulation curve, and the evaporation efficiency of MG-Si was higher than those of Si-S-L and Si-S samples.

ACKNOWLEDGEMENTS

We gratefully acknowledge the support of the National Science Foundation of China-Yunnan (U1137601), the National Natural Science Foundation of China Nos. 51334004 and 51204143, and the Scientific and Technological Innovation Platform of Fujian Province (2006L2003). Moreover, we thank Yanxu Lin for assistance with the samples.

REFERENCES

1. B.N. Mukashev, Kh.A. Abdullin, M.F. Tamendarov, T.S. Turmagambetov, B.A. Beketov, M.R. Page, and D.M. Kline, *Sol. Energy Mater. Sol. Cells* 93, 1785 (2009).
2. J.K. Lee, J.S. Lee, B.Y. Jang, J.S. Kim, Y.S. Ahn, G.H. Kang, H.E. Song, M.G. Kang, and C.H. Cho, *Sol. Energy* 115, 322 (2015).
3. M.A. Martorano, J.B.F. Neto, T.S. Oliveira, and T.O. Tsubaki, *Mater. Sci. Eng. B* 176, 217 (2011).

4. T. Yoshikawa and K. Morita, *ISIJ Int.* 47, 582 (2007).
5. J. Safarian and M. Tangstad, *Metall. Mater. Trans. B* 43, 1427 (2012).
6. S.S. Zheng, T. Abel Engh, M. Tangstad, and X.T. Luo, *Sep. Purif. Technol.* 82, 128 (2011).
7. T. Ikeda and M. Maeda, *ISIJ Int.* 32, 635 (1992).
8. Y. Tan, X. Guo, S. Shi, W. Dong, and D.C. Jiang, *Vacuum* 93, 65 (2013).
9. S. Shi, W. Dong, X. Peng, D. Jiang, and Y. Tan, *Appl. Surf. Sci.* 266, 344 (2013).
10. L. Hu, Z. Wang, X. Gong, Z. Guo, and H. Zhang, *Metall. Mater. Trans. B* 44, 828 (2013).
11. D. Min and N. Sano, *Metall. Mater. Trans. B* 19, 433 (1988).
12. M.D. Johnston and M. Barati, *Sep. Purif. Technol.* 107, 129 (2013).
13. T.H. Ludwig, E. Schonhovd Dæhlen, P.L. Schaffer, and L. Arnberg, *J. Alloys Compd.* 586, 180 (2014).
14. L.A.V. Teixeira, Y. Tokuda, T. Yoko, and K. Morita, *ISIJ Int.* 49, 777 (2009).
15. J. Park, D. Min, and H. Song, *Metall. Mater. Trans. B* 33, 723 (2002).
16. L.A.V. Teixeira and K. Morita, *ISIJ Int.* 49, 783 (2009).
17. A. Tagaya, H. Chiba, F. Tsukihashi, and N. Sano, *Metall. Mater. Trans. B* 22, 499 (1991).
18. E.J. Jung, B.M. Moon, and D.J. Min, *Sol. Energy Mater. Sol. Cells* 95, 1779 (2011).
19. Y.V. Meteleva-Fischer, Y.X. Yang, R. Boom, B. Kraaijveld, and H. Kuntzel, *JOM* 64, 957 (2012).
20. K. Tang, E.J. Ovrelid, G. Tranell, and M. Tangstad, *Mater. Trans.* 50, 1978 (2009).
21. K. Morita, *Modeling, Control and Optimization in Ferrous and Nonferrous Industry* (Warrendale, PA, 2003).
22. T. Shimpo, T. Yoshikawa, and K. Morita, *Metall. Mater. Trans. B* 35, 277 (2004).
23. E.T. Turkdogan, *Physical Chemistry of High Temperature Technology* (New York: Academic Press, 1980).
24. K. Morita, K. Kume, and N. Sano, *Scand. J. Metall.* 31, 178 (2002).
25. T. Miki, K. Morita, and N. Sano, *Metall. Mater. Trans. B* 27B, 937 (1996).
26. E.T. Turkdogan, *ISIJ Int.* 40, 964 (2000).
27. I.H. Jung and Y. Zhang, *JOM* 64, 973 (2012).
28. S. Tabuchi and N. Sano, *Metall. Mater. Trans. B* 15, 351 (1984).
29. C.H. Lupis, Elsevier Science Publishing Co., Inc., 1983, p. 581.
30. M. Fang, C.H. Lu, L.Q. Huang, H.X. Lai, J. Chen, J.T. Li, W.H. Ma, P.F. Xing, and X.T. Luo, *Ind. Eng. Chem. Res.* 53, 972 (2014).
31. J.P. Martins and F. Margarido, *Mater. Chem. Phys.* 44, 156 (1996).
32. E. Machlin, *Trans. Am. Inst. Min. Metall. Pet. Eng. Soc. Min. Eng. AIME* 218, 314 (1960).
33. K. Tang, E.J. Øvrelid, G. Tranell, and M. Tangstad, *JOM* 61, 49 (2009).
34. J. Szekely, C. Chang, and W. Johnson, *Metall. Mater. Trans. B* 8, 514 (1977).
35. D.C. Jiang, S.Q. Ren, S. Shi, W. Dong, J.S. Qiu, Y. Tan, and J.Y. Li, *J. Electron. Mater.* 43, 314 (2014).
36. S.S. Zheng, T.A. Engh, M. Tangstad, and X.T. Luo, *Metall. Mater. Trans. A* 42, 2214 (2011).